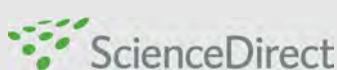
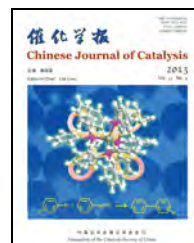


available at [www.sciencedirect.com](http://www.sciencedirect.com)journal homepage: [www.elsevier.com/locate/chnjc](http://www.elsevier.com/locate/chnjc)**Article****Methanol electro-oxidation on a porous nanostructured Ni/Pd-Ni electrode in alkaline media**

Mir Ghasem Hosseini\*, Mehdi Abdolmaleki, Sajjad Ashrafpoor

Electrochemistry Research Laboratory, Department of Physical Chemistry, Chemistry Faculty, University of Tabriz, Tabriz, Iran

**ARTICLE INFO****Article history:**

Received 13 April 2013

Accepted 17 June 2013

Published 20 September 2013

**Keywords:**

Methanol electro-oxidation

Palladium nanoparticle

Galvanic replacement

Cyclic voltammetry

Electrochemical impedance spectroscopy

Direct methanol fuel cell

**ABSTRACT**

A nanostructured Ni/Pd-Ni catalyst with high activity for methanol oxidation in alkaline solution was prepared by electrodeposition followed by galvanic replacement, that is, electrodeposition of Ni-Zn on a Ni coating with subsequent replacement of the Zn by Pd at the open circuit potential in a Pd-containing alkaline solution. The surface morphology and composition of the coatings were examined by energy dispersive X-ray spectroscopy and scanning electron microscopy. The Ni/Pd-Ni coatings were porous and were composed of discrete Pd nanoparticles of about 58 nm. The electrocatalytic activity of the Ni/Pd-Ni electrodes for the oxidation of methanol was examined by cyclic voltammetry and electrochemical impedance spectroscopy. The onset potentials for methanol oxidation on Ni/Pd-Ni were 0.077 V and 0.884 V, which were lower than those for flat Pd and smooth Ni electrodes, respectively. The anodic peak current densities of these electrodes were 4.33 and 8.34 times higher than those of flat Pd ( $58.4 \text{ mA/cm}^2$  vs  $13.47 \text{ mA/cm}^2$ ) and smooth Ni ( $58.4 \text{ mA/cm}^2$  vs  $7 \text{ mA/cm}^2$ ). The nanostructured Ni/Pd-Ni electrode is a promising catalyst for methanol oxidation in alkaline media for fuel cell application.

© 2013, Dalian Institute of Chemical Physics, Chinese Academy of Sciences.

Published by Elsevier B.V. All rights reserved.

**1. Introduction**

In recent years, much attention has been paid to direct alcohol fuel cells (DAFCs) for portable application for their advantages over hydrogen fuel cells [1,2]. The most common DAFC is the direct methanol fuel cell (DMFC). Much work has been performed on the electro-oxidation of methanol and ethanol with various catalysts. Pt and Pt-based catalysts are the commonly used catalysts in acidic medium [3–5], but Pt-based anodes in acidic medium undergo inevitable deactivation due to poisoning by the reaction intermediates, particularly CO, and so the high cost of Pt-based electrocatalysts and the scarcity of Pt limited their commercial application. Many non-platinum metals have been studied in alkaline media [6–10]. Pd is the most attractive possible replacement for Pt because Pd is ra-

ther low cost compared to Pt [11]. More importantly, unlike Pt-based metals and alloys, Pd-based electrocatalysts are highly active for the oxidation of a large variety of substrates in an alkaline environment [12–14]. In alkaline media, a number of non-noble metals are also sufficiently stable and can be incorporated with Pd to enhance its catalytic efficiency for alcohol oxidation and poison tolerance.

The catalytic activity of Pd can be modified by alloying it with other metals, among which Ni has been the main focus. Liu et al. [15] synthesized Pd-Ni nanoparticles by chemical reduction with formic acid. Both electrodeposited bimetallic Pd-Ni film [16] and Pd-Ni alloy [17] showed enhanced catalytic activity as compared with pure Pd synthesized by the same process. In addition, alloying of Pd with Ni further enhanced the tolerance of Pd to poisoning because Ni is an oxophilic element [18].

\*Corresponding author. Tel: +98-41-13393138; Fax: +98-41-13340191; E-mail: mg-hosseini@tabrizu.ac.ir; mirghasem@yahoo.com

This work was supported by Iran National Science Foundation and the financial support of the Office of Vice Chancellor in Charge of Research of University of Tabriz.

DOI: 10.1016/S1872-2067(12)60643-3 | <http://www.sciencedirect.com/science/journal/18722067> | Chin. J. Catal., Vol. 34, No. 9, September 2013

Recently, there was considerable interest in porous bimetallic nanostructures because of their high specific surface, low density, and reduced cost [19–22]. Many bimetallic catalysts can achieve higher activity and stability than the monometallic ones. The galvanic replacement reaction provides a very simple and effective method to prepare porous bimetallic nanostructures with a lower standard electrode potential than the target material.

Here we demonstrate a protocol for the synthesis of porous Ni/Pd-Ni nanostructures by galvanic replacement reaction using Zn from a Ni/Zn-Ni coating. The Ni-Zn coating was formed on Ni by electrodeposition and a Ni/Zn-Ni electrode was obtained. Porous Ni/Pd-Ni nanostructures were produced by exposing the Ni/Zn-Ni electrode to an alkaline aqueous solution of the corresponding palladium salt (0.001 mol/L PdCl<sub>2</sub> + 30% NaOH). These porous nanostructures were stable at ambient conditions and showed a highly porous catalytic surface that is suitable for the electro-oxidation of methanol in alkaline solution.

## 2. Experimental

### 2.1. Catalyst preparation

All reagents used were analytical grade and provided by Merck. They were used without further purification. For each experiment, a freshly prepared electrode and solution were used. The Ni/Pd-Ni catalysts were prepared by electrodeposition and galvanic replacement. The preparation schemes for the smooth nickel and nanostructured Ni/Pd-Ni electrodes are presented in Fig. 1. The copper electrodes were cut and mounted in a polyester resin except for a surface area of 1 cm<sup>2</sup> exposed for measurements. The electrical connection was provided by a copper wire. Before electrodeposition, the electrode surfaces were polished with emery paper (2500 grit size),

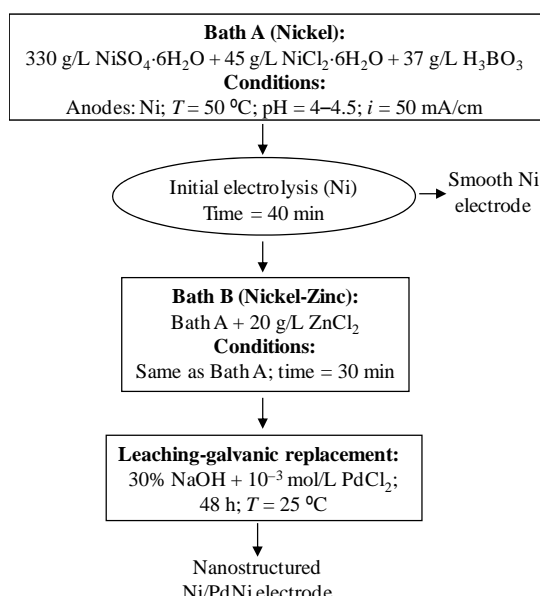
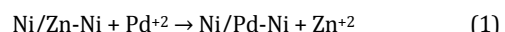


**Fig. 1.** Scheme of preparation procedure for the smooth Ni and nanostructured Ni/Pd-Ni electrodes.

washed with distilled water, thoroughly degreased in a 30% NaOH solution for 5 min, washed again with distilled water, dipped into 10% H<sub>2</sub>SO<sub>4</sub> solution for 1 min, followed by a wash with distilled water and then immersed in the bath solution.

After deposition, the electrodes were rinsed with distilled water to remove residual bath chemicals and unattached particles. Pd deposition was performed simply by dipping the Ni/Zn-Ni electrode into a 30% NaOH solution of PdCl<sub>2</sub> salt of concentration 0.001 mol/L for 48 h at room temperature. The plating baths and conditions used for the smooth Ni and Ni/Zn-Ni coatings are illustrated in Fig. 1.

The standard reduction potential of the Pd<sup>+2</sup>/Pd pair (0.83 V vs SHE) is higher than the reduction potential of the Zn<sup>+2</sup>/Zn pair (-0.762 V vs SCE), so it can be reduced by Zn in the reaction



Finally, the electrode was removed from the solution and washed with pure water.

### 2.2. Catalyst characterization

The morphology of the samples was studied by a scanning electron microscope (SEM, Philips Model XL30). The composition of the samples was determined by energy dispersive X-ray spectroscopy (EDX) experiments, which were carried out on the same SEM apparatus.

### 2.3. Electrochemical studies

Electrochemical studies were carried out in a conventional electrochemical cell. All solutions were purged with purified nitrogen for 10 min before the measurements. A standard three-electrode cell arrangement was used in all experiments. A platinum sheet with a geometric area of 20 cm<sup>2</sup> was used as the counter electrode and all potentials were measured versus a commercial saturated calomel electrode (SCE). Cyclic voltammetry (CV) and electrochemical impedance spectroscopy (EIS) studies were performed using a Princeton Applied Research, EG&G PARSTAT 2263 Advanced Electrochemical system run by the PowerSuite software. The CV of each electrocatalyst was measured between -1.5 and +0.75 V (vs SCE) in 1 mol/L NaOH with and without methanol at 298 K. The impedance spectra were recorded between the frequency range of 100 kHz and 10 mHz, with the amplitude (r.m.s value) of the ac signal being 10 mV. The data were curve fitted and analyzed using the ZView(II) software.

## 3. Results and discussion

### 3.1. Characterization results of the coatings

The SEM images of the smooth Ni, Ni/Zn-Ni, and Ni/Pd-Ni electrodes are shown in Fig. 2. The smooth Ni electrode showed a relatively homogeneous surface with small roughness and can be considered a quasi-two dimensional surface (Fig. 2(a)). It can be seen from Fig. 2(b) that the Ni surface was fully covered by the Ni-Zn layer. The Ni/Zn-Ni coating was compact and

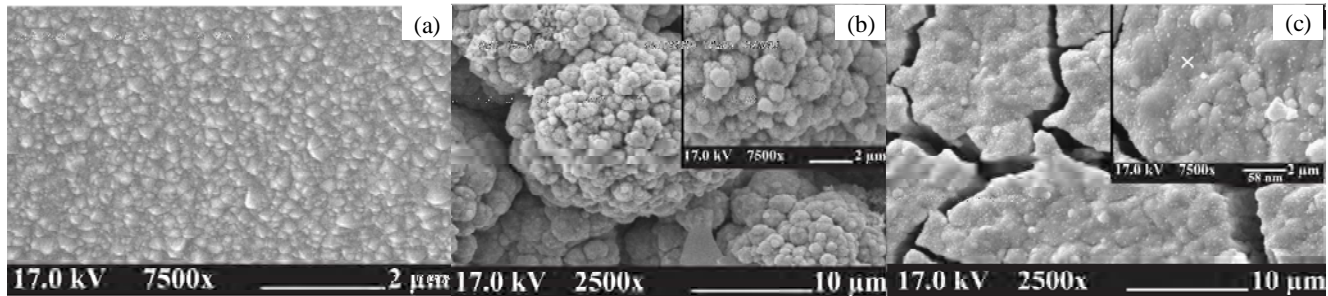


Fig. 2. SEM images of the surfaces of smooth Ni (a), Ni/Zn-Ni coating (b), and Ni/Pd-Ni coating after the leaching-galvanic replacement process (c).

has a porous structure. However, the morphology of the surface changed significantly after the leaching-galvanic replacement of Zn in the deposit (Fig. 2(c)). A large number of cracks and pores appeared, giving a high surface area for the methanol oxidation reaction. The Ni/Pd-Ni deposits were nano-particulate (approximately 58 nm) in nature with a high coverage of the substrate.

The surface EDX spectra of the electrodes are given in Fig. 3. The EDX analysis showed that the chemical composition of the surface before leaching-replacement was 16.87 at% Ni and 83.13 at% Zn. After the alkaline leaching-galvanic replacement, the surface composition was changed to be 24.94 at% Ni, 59.52 at% Zn and 15.54 at% Pd (Fig. 3(b)). The chemical composition analysis revealed that the Zn content was decreased considerably by the selective dissolution, which led to pore and crack formation that produced a highly porous surface suitable for methanol electro-oxidation. Also, as is evident from Fig. 3, the EDX results confirmed the presence of palladium nanoparticles on the surface film.

### 3.2. Cyclic voltammetry

The electrocatalytic activity of the smooth Ni, flat Pd, and nanostructured Ni/Pd-Ni electrodes for methanol oxidation was evaluated by cyclic voltammetry. Figure 4 shows typical CVs during methanol electro-oxidation on these electrodes in 1 mol/L NaOH solution containing 0.1 mol/L methanol at room

temperature. The CVs of the above electrodes in 1 mol/L NaOH in the absence of methanol under the same conditions are shown in the insets of Fig. 4. The potential was swept between -1.5 and 0.75 V versus SCE at a scan rate of 10 mV/s during the experiments.

By comparison with the CV from the smooth Ni electrode in 1 mol/L NaOH, the reduction current peaks of palladium oxide can be clearly observed from the flat Pd and Ni/Pd-Ni catalysts (Fig. 4(b) and (c)). The electro-oxidation of methanol on the smooth Ni and porous Ni/Zn-Ni electrodes in the presence and absence of methanol in the 1 mol/L NaOH solution has been described in detail in our previous publication [22]. In brief, methanol oxidation takes place after the oxidation of  $\text{Ni}(\text{OH})_2$  to  $\text{NiOOH}$  [23,24]. The  $\text{Ni}^{2+}/\text{Ni}^{3+}$  redox couple acts as a catalyst for the oxidation of methanol in basic solutions. Therefore, for the smooth Ni electrode, the first peak (0.39 V vs SCE) was the  $\alpha\text{-Ni}(\text{OH})_2/\text{NiOOH}$  redox couple and the other peak (0.525 V vs SCE) was assigned to methanol electro-oxidation. The peak current density was 7 mA/cm<sup>2</sup>.

Methanol electro-oxidation on the flat Pd and Ni/Pd-Ni electrodes were characterized by two well-defined current peaks in the forward and reverse scans. In the forward scan, the oxidation peak corresponded to the oxidation of freshly chemisorbed species from methanol adsorption [25,26]. The reverse scan peak was primarily associated with the removal of carbonaceous species not completely oxidized in the forward scan and not to the oxidation of freshly chemisorbed species

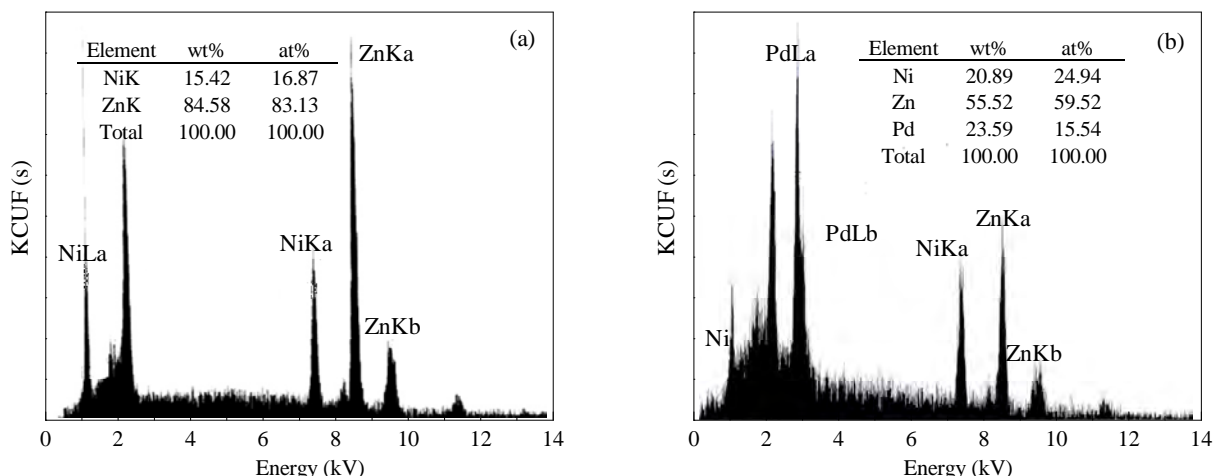
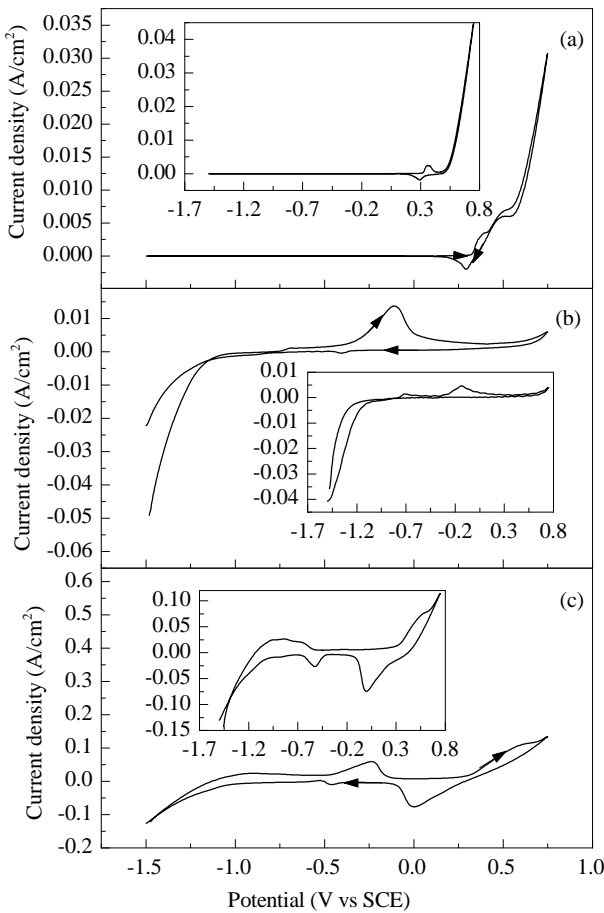


Fig. 3. EDX spectra obtained from the surfaces of Ni/Zn-Ni electrode (a) and Ni/Pd-Ni electrode after leaching-galvanic replacement process (b).



**Fig. 4.** Cyclic voltammograms of smooth Ni electrode (a), flat Pd electrode (b), and nanostructured Ni/Pd-Ni electrode (c) in a 1 mol/L NaOH solution containing 0.1 mol/L methanol at a potential scan rate of 10 mV/s, and the cyclic voltammograms without methanol in the 1 mol/L NaOH solution at the scan rate of 10 mV/s are shown in the insets.

[27–30]. However, the assignment of the reverse scan peak is still under debate.

As shown in Fig. 4, the forward peak potential for the electro-oxidation of methanol on the nanostructured Ni/Pd-Ni electrode was −0.226 V (vs SCE), which was lower than −0.096 V (vs SCE) for flat Pd and lower than 0.525 V (vs SCE) for the smooth Ni electrode. Also, the peak current densities associated with methanol oxidation in the forward scan for Ni/Pd-Ni, flat Pd, and smooth Ni were 58.4, 13.47, and 7 mA/cm<sup>2</sup>, respectively. The electrocatalytic activity was therefore in the order smooth Ni < flat Pd < Ni/Pd-Ni. The large peak oxidation current and low anodic peak potential showed that the Ni/Pd-Ni electro-catalyst was more active than the flat Pd and smooth Ni electrodes. This finding confirmed that the leaching-galvanic replacement method provided a highly active electrochemical active area for methanol electrooxidation. Moreover, the higher catalytic currents at more negative potentials on the Ni/Pd-Ni electro-catalysts would improve DMFC efficiency. The effect of scan rate on the cyclic voltammetry behavior of the porous Ni/Pd-Ni nanostructured electrode in 1 mol/L NaOH/0.1 mol/L methanol solution is shown in Fig. 5(a). Plots of the forward

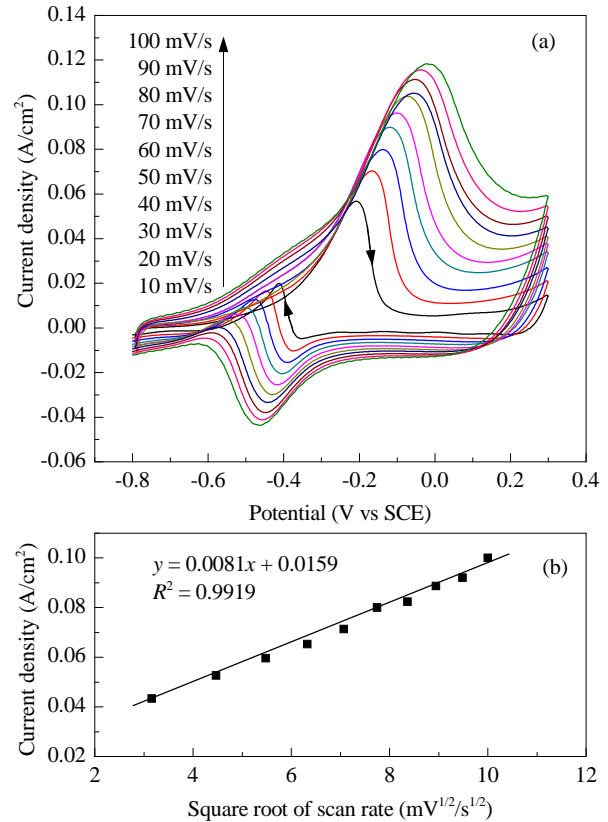


**Fig. 5.** (a) Cyclic voltammograms for the nanostructured Ni/Pd-Ni electrode in 1 mol/L NaOH + 0.1 mol/L CH<sub>3</sub>OH at different scan rates; (b) Methanol oxidation peak current on the porous Ni/Pd-Ni electrode versus square root of the scan rate.

peak current density versus square root of the scan rate for the Ni/Pd-Ni electrode are given in Fig. 5(b). The forward peak current density showed a linear increase with the square root of the scan rate, indicating a diffusion-controlled electrocatalytic oxidation process (Fig. 5(b)). The forward peak potential was also more shifted to positive values with the square root of the scan rate, showing that an irreversible electrode reaction took place on the Ni/Pd-Ni electrode surface.

Figure 6(a) shows typical CVs for the Ni/Pd-Ni electrode as a function of CH<sub>3</sub>OH concentration between 0.1 and 0.7 mol/L. The forward peak potential was shifted slightly toward more positive values with increasing CH<sub>3</sub>OH concentration. The peak current density increased linearly with concentration, as shown in Fig. 6(b). The slope of this straight line is the order of reaction with respect to methanol according to the relations [31]:

$$\text{Rate} \equiv I_p = kc^n, \log I_p = \log k + n \log c \quad (2)$$

where  $I_p$  is the peak current density,  $k$  is the reaction rate constant,  $c$  is the bulk concentration of methanol, and  $n$  is the reaction order. The reaction rate constant and reaction order values on the nanostructured Ni/Pd-Ni electrode were 5.107 and 0.5684, respectively (Fig. 6(c)). For methanol oxidation, there was an optimum activity at the concentration of 0.6 mol/L. When the methanol concentration exceeded 0.6 mol/L, the peak current slightly increased. The comparison of the catalytic activity of the Ni/Pd-Ni electrode with the different Ni-Pd elec-

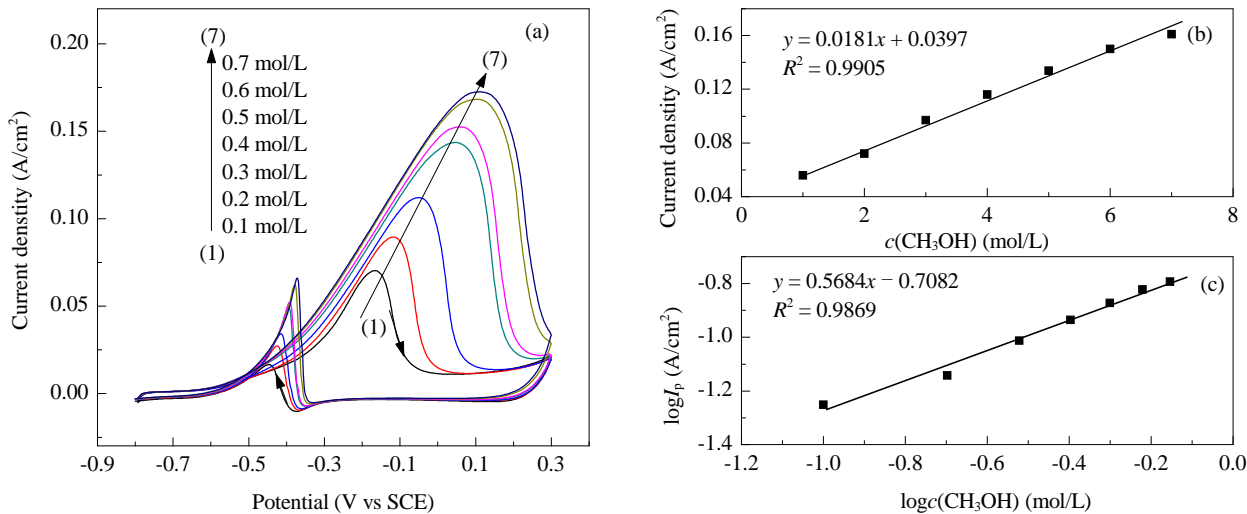


**Fig. 6.** (a) Cyclic voltammograms of the porous Ni/Pd-Ni electrode from  $-0.8$  to  $0.3$  V versus SCE at the scan rate of  $20$  mV/s for different methanol concentrations; (b) Methanol oxidation peak current on the porous Ni/Pd-Ni electrode versus methanol concentration; (c)  $\log I_p$ - $\log c$  curves obtained with the Ni/Pd-Ni electrode at  $10$  mV/s scan rate.

trodes in the literature revealed that the peak current density for methanol oxidation on the nanoporous Ni/Pd-Ni electrode was higher than that of the different Ni-Pd electrodes [16,18,32,33]. Therefore, the Ni/Pd-Ni catalyst is a promising anode electrocatalyst for the direct methanol fuel cell.

In order to study the dependence of the electrocatalytic performance of Ni/Pd-Ni electrode on electrolyte temperature, the effect of temperature on methanol oxidation on the Ni/Pd-Ni electrode was investigated in the temperature range of  $308$ – $338$  K by cyclic voltammetry. From Fig. 7, it can be seen that the anodic current increased with temperature. Furthermore, some special behavior was also observed in methanol oxidation, such as a positive shift in the forward anodic oxidation and reverse peak potential, and a negative shift at the onset potential. With the increase in temperature, the differences in the onset potentials became smaller. Figure 7(b) shows the Arrhenius plot of  $\ln i$  versus  $T^{-1}$  for the Ni/Pd-Ni electrode. The apparent activation energy calculated from the slope of the plot was  $11.55$  kJ/mol. As the temperature increased, the electro-oxidation current density increased. This was attributed to the increase in the rate of charge transfer at the electrode/electrolyte interface.

### 3.3. EIS results

The Nyquist plots and equivalent electrical circuits of the impedance of the Ni/Pd-Ni electrode for methanol electro-oxidation at different potentials in  $1$  mol/L NaOH/ $0.1$  mol/L methanol solution are shown in Figs. 8 and 9, respectively.

The Nyquist plots presented in Fig. 8 suggest porosity in the electrode surfaces. Typically, Nyquist plots of porous electrodes show either a line with a slope of  $45^\circ$  or a semicircle at high frequencies followed by a semicircle at low frequencies [34,35]. The impedance data from the electro-oxidation of  $\text{CH}_3\text{OH}$  at the Ni/Pd-Ni electrode were fitted using the equivalent circuits

shown in Fig. 9. The symbols  $R_s$ ,  $R_p$ ,  $R_{ct}$ , and  $R_1$  represented the solution, pore, charge transfer, and adsorption resistances, respectively, CPE<sub>p</sub> and CPE<sub>dl</sub> represented the constant phase elements (CPE) for the porous electrode and the catalyst/solution interface, respectively, and L represented an inductance used to account for the impedance contribution of the adsorption and desorption taking place at the composite elec-

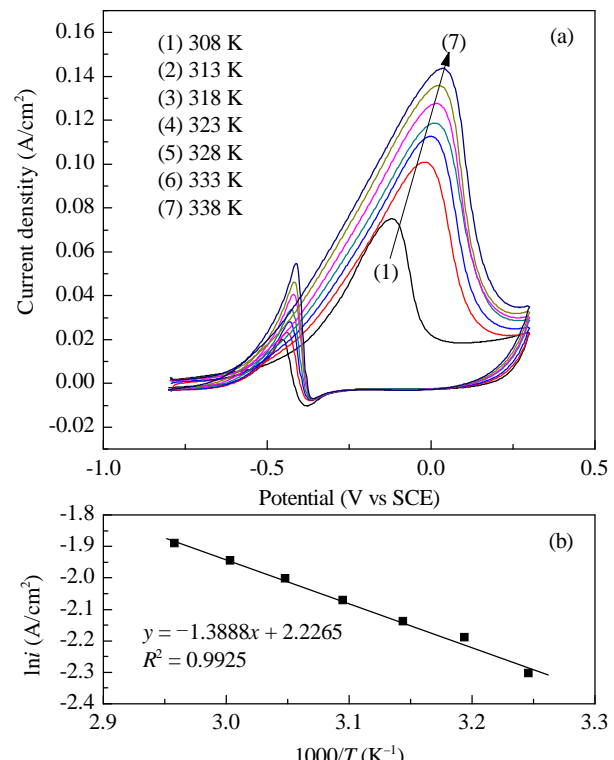


**Fig. 7.** (a) Effect of temperature on cyclic voltammograms of methanol oxidation on Ni/Pd-Ni electrode in the range of  $308$ – $338$  K in  $1$  mol/L NaOH +  $0.1$  mol/L  $\text{CH}_3\text{OH}$  solution; (b) Arrhenius plot for methanol oxidation on the Ni/Pd-Ni electrode.

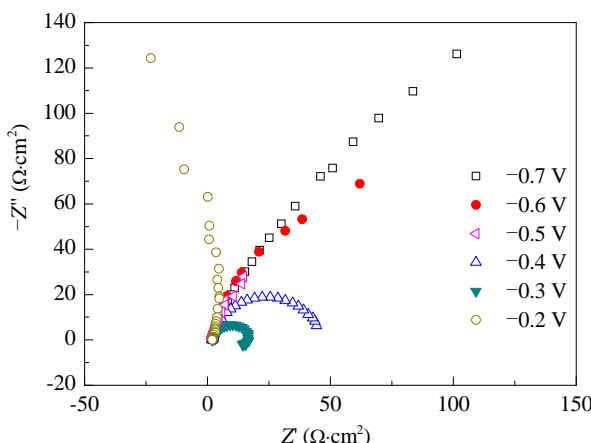


**Fig. 8.** Experimental Nyquist diagrams as a function of applied potential for methanol electro-oxidation on nanoporous Ni/Pd-Ni electrode in 1 mol/L NaOH/0.1 mol/L methanol aqueous solution.

trode at low frequencies [36,37].

The CPE is defined by two parameters,  $T$  and  $\phi$ , in the equation for impedance [38]:

$$Z_{\text{CPE}} = 1/T(j\omega)^\phi \quad (3)$$

where  $Z_{\text{CPE}}$  is constant phase element impedance,  $T$  is the admittance factor, and  $\phi$  is the phase shift, which can be explained as a degree of surface inhomogeneity. The EIS results indicated that methanol electro-oxidation on the nanostructured Ni/Pd-Ni catalyst at various potentials showed different impedance behavior. A large depressed arc shown in the potential between -0.7 and -0.4 V versus SCE revealed a slow reaction rate of methanol dehydrogenation [39]. As can be clearly seen in Fig. 8, with the increase of anodic potential, the diameter of the depressed arc decreased rapidly, indicating

that the charge transfer resistance for the methanol electro-oxidation became smaller. This was because the onset potential for a current rise for methanol electro-oxidation on the nanostructured Ni/Pd-Ni electrode was -0.474 V versus SCE (Fig. 4(c)).

At the potential of -0.3 V versus SCE, a so-called 'pseudo-inductive' behavior began to emerge in the impedance plot, where two large positive loops at a higher frequency was accompanied by a small loop in the fourth quadrant at low frequency. The latter can be attributed to enhanced desorption of the adsorbed reaction intermediate (CO) from the electrode surface. Desorption can increase the active sites and hence, the rate of methanol oxidation reaction [40]. Another explanation for the occurrence of the inductive behavior during methanol electro-oxidation would be that it was due to the removal of adsorbed intermediates and creation of sites for further adsorption and reaction [41]. Generally, the so-called 'pseudo-inductive' behavior results from a 'relaxation phenomenon' between adsorption-dehydrogenation of methanol molecules and oxidation-adsorption of the CO-like species.

As the potential reached -0.2 V versus SCE, a sudden change in the impedance plots occurred, with the loop reversing to the second quadrant as shown in Fig. 8. The main reason is that the electrochemical reaction changed from methanol dehydrogenation to the oxidation and removal of  $\text{CO}_{\text{ads}}$  by  $\text{OH}_{\text{ads}}$ , which led to the reversal of impedance in the second quadrant [39]. These observations are consistent with the CV results.

The equivalent circuit shown in Fig. 9(a) was developed to fit the above impedance data at the potentials of -0.7, -0.6, -0.5, -0.4, and -0.2 V versus SCE. The equivalent circuit shown in Fig. 9(b) was used to fit the impedance data at the potential of -0.3 V versus SCE. Table 1 shows the values of the equivalent

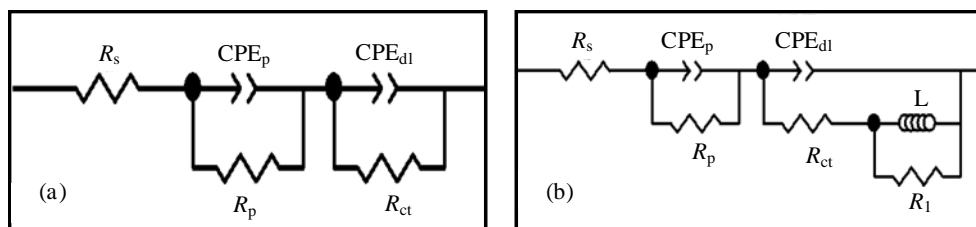


**Fig. 9.** Equivalent circuits for the electro-oxidation of methanol at the Ni/Pd-Ni electrode in varied potential regimes. (a) At potentials -0.7, -0.6, -0.5, -0.4, and -0.2 vs SCE; (b) At potential -0.3 V vs SCE.

**Table 1**

Equivalent circuit parameters of the electro-oxidation of 0.1 mol/L methanol on the nanoporous Ni/PdNi electrode in 1 mol/L NaOH solution obtained from Fig. 8.

Element	-0.7 V vs SCE	-0.6 V vs SCE	-0.5 V vs SCE	-0.4 V vs SCE	-0.3 V vs SCE	-0.2 V vs SCE
$R_s (\Omega \cdot \text{cm}^2)$	1.88	1.96	1.96	1.96	1.96	1.98
$T_p (\text{s}^\phi \Omega^{-1} \cdot \text{cm}^{-2})$	0.06546	0.08441	0.2921	0.2364	0.00697	0.37539
$\phi_p$	0.76	0.75	0.61	0.64	0.5	0.57
$R_p (\Omega \cdot \text{cm}^2)$	30.52	14.37	2.13	2.56	1.06	0.57
$T_{dl} (\text{s}^\phi \Omega^{-1} \cdot \text{cm}^{-2})$	0.0597	0.03395	0.07122	0.02888	0.03563	0.09188
$\phi_{dl}$	1	1	1	0.95	0.89	0.97
$R_{ct} (\Omega \cdot \text{cm}^2)$	215.4	120.8	67.96	40.63	10.25	-338.1
$L (\text{H})$	—	—	—	—	27.79	—
$R_1 (\Omega \cdot \text{cm}^2)$	—	—	—	—	6.28	—
Error (%)	3.59	4.57	3.414	2.32	2.25	6.89

circuit elements obtained by fitting to the experimental results. The mean error was smaller than 7%, indicating a good fit of the experimental data.

#### 4. Conclusions

A new porous Ni/Pd-Ni nanocatalyst was prepared by a simple galvanic replacement reaction of Ni/Zn-Ni in an alkaline palladium solution. The electro-oxidation of CH<sub>3</sub>OH in 1 mol/L NaOH solution by the Ni/Pd-Ni electrode was studied by CV and EIS. The results were compared to those from flat Pd and smooth Ni electrodes. SEM results showed that the Pd nanoparticles in the Ni/Pd-Ni catalyst were highly dispersed and the alkaline leaching-galvanic replacement process produced a highly porous catalytic surface that is suitable for the electro-oxidation of methanol. The methanol oxidation reaction onset potential on Ni/Pd-Ni (-0.474 V vs SCE) was shifted 0.884 and 0.077 V toward more negative values compared to those for smooth Ni and flat Pd electrodes, respectively. The comparison of the flat Pd, smooth Ni, and porous Ni/Pd-Ni electrodes showed that the current density for methanol oxidation on the Ni/Pd-Ni electrode (58.4 mA/cm<sup>2</sup>) were higher than those on the flat palladium (13.47 mA/cm<sup>2</sup>) and smooth Ni electrodes (7 mA/cm<sup>2</sup>). This was because the Ni/Pd-Ni electrode has smaller metal particles, leading to a larger surface area. Therefore, the Ni/Pd-Ni catalyst would be suitable as the anodic catalyst for the direct methanol fuel cell. The EIS responses were strongly dependent on electrode potential. The EIS measurements were consistent with the results from cyclic voltammetry and confirmed the porosity of the Ni/Pd-Ni electrode.

#### References

- [1] Hosseini M G, Momeni M M. *Electrochim Acta*, 2012, 70: 1
- [2] Tang S H, Sun G Q, Qi J, Sun S G, Guo J S, Xin Q, Haarberg G M. *Chin J Catal* (催化学报), 2010, 31: 12
- [3] Wang X Y, Zhang J C, Zhu H. *Chin J Catal* (催化学报), 2011, 32: 74
- [4] Ma J H, Feng Y Y, Zhang G R, Wang A J, Xu B Q. *Chin J Catal* (催化学报), 2010, 31: 521
- [5] Zhou C M, Wang H J, Liang J H, Peng F, Yu H, Yang J. *Chin J Catal* (催化学报), 2008, 29: 1093
- [6] Jafarian M, Moghaddam R B, Mahjani M G, Gobal F. *J Appl Electrochem*, 2006, 36: 913
- [7] Jafarian M, Mahjani M G, Heli H, Gobal F, Khajehsharifi H, Hamed M H. *Electrochim Acta*, 2003, 48: 3423
- [8] Cubeiro M L, Fierro J L G. *Appl Catal A*, 1998, 168: 307
- [9] Chen Y G, Zhuang L, Lu J T. *Chin J Catal* (催化学报), 2007, 28: 870
- [10] Heli H, Jafarian M, Mahjani M G, Gobal F. *Electrochim Acta*, 2004, 49: 4999
- [11] *Platinum Metals Rev*, 2009, 53: 48
- [12] Xu C W, Tian Z Q, Shen P K, Jiang S P. *Electrochim Acta*, 2008, 53: 2610
- [13] Xu C W, Shen P K, Liu Y L. *J Power Sources*, 2007, 164: 527
- [14] Hosseini M G, Momeni M M, Khalilpur H. *Int J Nanosci*, 2012, 11: 1250016
- [15] Liu Z L, Zhang X H, Hong L. *Electrochim Commun*, 2009, 11: 925
- [16] Qiu C C, Shang R, Xie Y F, Bu Y R, Li C Y, Ma H Y. *Mater Chem Phys*, 2010, 120: 323
- [17] Du C Y, Chen M, Wang W G, Yin G P, Shi P F. *Electrochim Commun*, 2010, 12: 843
- [18] Qi Z, Geng H R, Wang X G, Zhao C C, Ji H, Zhang C, Xu J L, Zhang Z H. *J Power Sources*, 2011, 196: 5823
- [19] Hosseini M G, Abdolmaleki M, Ashrafpoor S. *Chin J Catal* (催化学报), 2012, 33: 1817
- [20] Solmaz R, Döner A, Şahin İ, Yüce A O, Kardaş G, Yazıcı B, Erbil M. *Int J Hydrogen Energy*, 2009, 34: 7910
- [21] Hosseini M G, Abdolmaleki M. *Int J Hydrogen Energy*, 2013, 38: 5449
- [22] Hosseini M G, Abdolmaleki M, Ashrafpoor S. *J Appl Electrochem*, 2012, 42: 153
- [23] Vértes G, Horányi G. *J Electroanal Chem Interf Electrochem*, 1974, 52: 47
- [24] Robertson P M. *J Electroanal Chem Interf Electrochem*, 1980, 111: 97
- [25] Xu C W, Liu Y L, Yuan D S. *Int J Electrochem Sci*, 2007, 2: 674
- [26] Lee Y W, Han S B, Park K W. *Electrochim Commun*, 2009, 11: 1968
- [27] Singh R N, Singh A, Anindita. *Int J Hydrogen Energy*, 2009, 34: 2052
- [28] Liu J P, Ye J Q, Xu C W, Jiang S P, Tong Y X. *Electrochim Commun*, 2007, 9: 2334
- [29] Xu M W, Gao G Y, Zhou W J, Zhang K F, Li H L. *J Power Sources*,

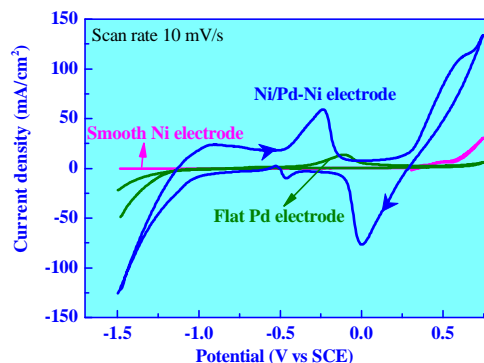
#### Graphical Abstract

*Chin. J. Catal.*, 2013, 34: 1712–1719 doi: 10.1016/S1872-2067(12)60643-3

#### Methanol electro-oxidation on a porous nanostructured Ni/Pd-Ni electrode in alkaline media

Mir Ghasem Hosseini\*, Mehdi Abdolmaleki, Sajjad Ashrafpoor  
University of Tabriz, Iran

The nanostructured Ni/Pd-Ni electrode shows significantly greater electro-catalytic activity towards methanol oxidation than flat palladium and smooth nickel electrodes. The high activity of Ni/Pd-Ni electrode can be attributed to its high surface area.



- 2008, 175: 217
- [30] Huang J C, Liu Z L, He C B, Gan L M. *J Phys Chem B*, 2005, 109: 16644
- [31] Beden B, Kadirgan F, Lamy C, Leger J M. *J Electroanal Chem Interf Electrochem*, 1982, 142: 171
- [32] Miao F J, Tao B R. *Electrochim Acta*, 2011, 56: 6709
- [33] Kumar K S, Haridoss P, Seshadri S K. *Surf Coat Technol*, 2008, 202: 1764
- [34] Hitz C, Lasia A. *J Electroanal Chem*, 2001, 500: 213
- [35] Lasia A. *J Electroanal Chem*, 1995, 397: 27
- [36] Birry L, Lasia A. *J Appl Electrochem*, 2004, 34: 735
- [37] Kubisztal J, Budniok A, Lasia A. *Int J Hydrogen Energy*, 2007, 32: 1211
- [38] Abdel-Rehim S S, Khaled K F, Abd-Elshafai N S. *Electrochim Acta*, 2006, 51: 3269
- [39] Hsing I M, Wang X, Leng Y J. *J Electrochem Soc*, 2002, 149: A615
- [40] Seland F, Tunold R, Harrington D A. *Electrochim Acta*, 2006, 51: 3827
- [41] Singh R N, Singh A, Anindita, Mishra D. *Int J Hydrogen Energy*, 2008, 33: 6878